UV to Near-IR CO Emissions from O + C_2H_2 and O + C_3O_2 Flames at Low Pressure and High Temperature†

Patti M. Sheaffer and Paul F. Zittel*

The Aerospace Corporation, P.O. Box 92957, Los Angeles, California 90009-2957

Received: March 31, 2000; In Final Form: June 1, 2000

Emission spectra from C_2H_2 + O flames have been studied in a low-pressure, fast flow discharge system under highly dilute, fuel-lean conditions from 295 to 873 K. Our previous work with room-temperature flames has been extended to look for temperature-induced changes in the relative populations of triplet CO(*a*), (*a*′), (*d*), and (*e*) reaction products by observing chemiluminescent emission in the 185−900 nm wavelength region. The effect of temperature on the relative yields of the CO triplet states was small, and the production rates increased linearly with the temperature-dependent rate of the initial O + C_2H_2 reaction step. To test the importance of C_2O as a major pathway to triplet state CO, similar experiments were performed on C_3O_2 + O flames. The relative yields of the CO triplet states showed little temperature dependence; however, the overall triplet production rate increased much faster with temperature than the initial O + C_3O_2 reaction and may be related to temperature variation of the branching ratio yielding C_2O in the initial reaction. Relative vibrational level populations were determined in the CO triplet states and were slightly hotter in C_3O_2 flames than in C_2H_2 flames throughout the temperature range.

1. Introduction

Emissions from electronically excited CO (CO*) are an important component of spectra from low-pressure hydrocarbon flames, but the chemical pathways from low molecular weight hydrocarbons to CO* are not fully understood. Although the Cameron CO(*a*→*X*), Asundi CO(*a*′→*a*), Triplet CO(*d*→*a*), and Herman CO(*e*→*a*) emission band systems in hydrocarbon flames have been reported in several studies, not all band systems are consistently observed. In our previous work,[1] extensive Cameron and Asundi emissions were observed for the first time in low-pressure, fuel-lean, highly dilute flames of acetylene (C_2H_2) and carbon suboxide (C_3O_2) with oxygen atoms (O). CO* triplet yields and vibrational distributions in the *a*, *a*′, *d* and *e* states were measured at room temperature with both fuels. Since triplet production is a relatively minor process in those flames at room temperature, the potential exists that at higher temperatures thermal energy may activate reaction pathways, or alter branching ratios, changing the CO* state distributions and overall triplet yields.

Burke et al.[1] demonstrated from the measured triplet CO* state distributions in room-temperature C_2H_2 + O and C_3O_2 + O flames that the CO(*a*) state, which gives rise to Cameron band emission, was most likely populated via radiative cascade from the higher triplet states. It was also found that within the limits of experimental error, the relative populations of all triplet states (i.e., *a*, *a*′, *d*, and *e*) were the same for C_2H_2 + O and C_3O_2 + O flames. The vibrational level distributions in a given triplet state were also nearly the same for both fuels. Thus, the same reaction mechanism was inferred for the production of CO* emission for both fuels, giving a strong indication that C_2O + O is the major reaction pathway in both reaction systems, at least at room temperature, as was inferred originally by Becker and Bayes.[2]

The primary thrust of the present work is to examine the combustion of C_2H_2 in O atom flames at elevated temperatures. The C_3O_2 + O reaction was also examined as a function of temperature since it appears that the only viable source of CO* in this system,

$$C_2O + O \rightarrow CO + CO^* \qquad \text{(r1)}$$

is also the main source of CO* emission when acetylene is burned in fuel-lean atomic oxygen flames.[1−6] The C_2H_2 + O reaction process is complex, giving rise to several precursors that could lead to CO*:

$$CH + O \rightarrow CO + H \qquad \Delta H = -176 \text{ kcal/mol} \qquad \text{(r2)}$$

$$CH_2 + O \rightarrow CO + H_2 \qquad \Delta H = -178 \text{ kcal/mol} \qquad \text{(r3)}$$

$$C_2O + O \rightarrow CO + CO \qquad \Delta H = -204 \text{ kcal/mol} \qquad \text{(r4)}$$

The exothermicity of reaction r4 is based on a value of $\Delta H^o_{f,298}(C_2O) = 92$ kcal/mol,[2,7] although other evaluations have suggested a value of 68.5 kcal/mol.[8] The exothermicities of reactions r2 and r3 are insufficient to populate the CO(*e*) state, so Herman band emissions are not expected unless significant contribution from reaction r4 is present. It has been observed that the Herman system is extensively populated in acetylene combustion,[1,2] which is consistent with reaction r4 being the primary source of CO* in room-temperature acetylene flames, although some participation of reactions r2 and r3 is not ruled out.

The production of triplet CO in C_2H_2 and C_3O_2 flames with O atoms is a relatively minor process at room temperature under low-pressure, fuel-lean conditions. The total yield of triplet CO(*a*, *a*′, *d*, and *e*) is approximately 4×10^{-4} to 5×10^{-3} per C_2H_2 molecule reacted and 7×10^{-5} to 1×10^{-3} per C_3O_2 molecule reacted.[1] The small yield is due both to small chemical yields of CO* precursors and small yields of electronically

† Part of the special issue "C. Bradley Moore Festschrift".

10.1021/jp001247l CCC: $19.00
Published on Web 07/11/2000

excited CO in the final reaction step. The important reactions and branching ratios, however, could be temperature dependent. First, from measurements in the C_3O_2 + O system,[1] the yield of CO* per C_2O + O reaction was estimated to be 3×10^{-3} to 5×10^{-2}. The somewhat uncertain[2,7,8] exothermicity of reaction r4 is only a little larger than the term energies of the CO (*d*) and (*e*) states (i.e., 175 and 184 kcal/mol, respectively). Thus, the small branching ratios to the different CO* states could be affected by thermal activation of the reactants. Second, the production of C_2O itself is a minor process with a direct yield reported to be <1% in the C_2H_2 + O reaction[9] and ~2.3% in the C_3O_2 + O reaction[10] at room temperature. The production of C_2O could have an activation energy greater than that of the main branch of the producing reaction in both flame systems, resulting in higher relative yields at higher temperatures. Third, it has been suggested on the basis of the relative CO* yields per C_2H_2 and C_3O_2 molecule that the C_2O in the C_2H_2 + O flame may come predominantly from the reaction of O atoms with the ketenyl (HCCO) radical.[11] HCCO is formed in the C_2H_2 + O reaction with a yield of 80 ± 15% nearly independent of temperature in the range of 290 to 1200 K.[5,12,13] A room-temperature branching fraction of ~11% into the C_2O-producing channel from the HCCO + O reaction has been postulated to explain the intensity of CO* emission in the C_2H_2 + O flame.[1] This minor branch of the reaction (the major products are 2CO + H) has not yet been substantiated. If this branch is important in overall C_2O formation, its temperature dependence would affect CO* yield at high temperatures. An example of the effect of temperature on branching fractions exists for a different minor channel of the HCCO + O reaction. Recently, a channel that produces CH($a^4\Sigma^-$ and $X^2\Pi$) was identified and found to increase with temperature from 6% of the total reaction at room temperature to 15% at 960 K, corresponding to an activation temperature of 560 K for the branch compared with 120 K for the total reaction.[14] Finally, precursors other than C_2O could be thermally activated to contribute to CO* production. CH and CH_2 in reactions r2 and r3 are apparently not important sources of CO* in fuel-lean, low-pressure C_2H_2 + O flames at room temperature, although the exothermicities are slightly larger than the threshold for producing CO(*d*) and not much below the threshold for CO(*e*). It is possible that the CO* yields of these reactions, as well as the relative rates of the reactions that produce CH and CH_2, could be enhanced at higher temperatures.

The production of C_2O in the C_3O_2 + O flame is an important element of our analysis of CO* emission. Two branches of the O atom reaction with C_3O_2 are[10,15]

$$C_3O_2 + O \rightarrow 3CO \qquad \Delta H = -116 \text{ kcal/mol} \qquad \text{(r5a)}$$

$$C_3O_2 + O \rightarrow C_2O + CO_2 \qquad \Delta H = -39.3 \text{ kcal/mol} \qquad \text{(r5b)}$$

where reaction r5a is the main branch at room temperature. Pilz and Wagner[15] saw little or no CO_2 as a gas-phase reaction product in their mass spectrometer measurement of the effluent of reaction r5 at low to moderately elevated temperatures. The implied branching fraction k_{5b}/k_5 was small (<1%) between 250 and 450 K. Williamson and Bayes[10] observed a 2.3 ± 0.5% yield of CO_2 from reaction r5 in room-temperature photolysis of dilute mixtures of N_2O and C_3O_2. Liuti et al.[18] reported a branching fraction of ~7% (with an uncertainty range of 3%−16%) from mass spectrometer measurements at room temperature. The somewhat uncertain branching fraction is apparently small at low temperatures, but could be different at higher temperatures.

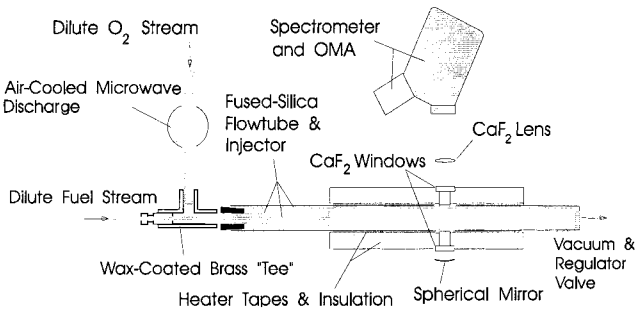

Figure 1. Diagram of the fast flow discharge system.

2. Experimental Section

2.1. Apparatus. Figure 1 shows a diagram of the fast flow discharge system (FFDS) heated flowtube. A 1 × 1 in. square quartz tube was heated with heavy-duty Nichrome heating tapes in two sections, upstream and downstream of the spectrometer viewing position. The heaters were independently monitored and controlled by chromel−alumel thermocouples sandwiched between the tube and heating elements. The chemiluminescence signal was observed through the walls of the quartz flowtube, which were comparable in transparency to quartz optical windows. The spectrometer viewed a narrow axial range of the hot zone through evacuated quartz inserts (with calcium fluoride outer windows), which were installed to avoid localized convective cooling of the viewing region by the ambient air.

All gas flows were fed through stainless steel lines and metered through MKS, Inc., mass flow controllers. O atoms were generated by passing 0.5% O_2 in Ar through a 40 W microwave discharge in a 12 mm diam quartz side tube. Surfaces between the discharge and heated section of the flowtube were coated with halocarbon wax to reduce O recombination. The O atom flows were determined before and after each run by titration with NO_2 upstream and downstream of the hot zone. Typical O atom flows were 0.9 to 1.3 sccm in 570 sccm Ar, with undissociated O_2 flows between 2.3 and 2.5 sccm. Acetylene and carbon suboxide flows were typically 0.18 and 0.29 sccm, respectively. The total pressure was 3 Torr in all runs. The velocity of the gas flow in room-temperature regions of the flowtube was 4 m/s and ranged from 4 to 12 m/s in the hot zone, depending on temperature.

Fuel (mixed in Ar) was injected 16 cm upstream of the spectrometer viewing position at the beginning of a hot zone. The quartz injector at the end of a sliding tube consisted of a cross with 4 arms extending 0.95 cm radially from the flowtube centerline and drilled with several 0.05 cm holes to inject fuel transverse to the main flow. The temperature in the hot zone was measured in the center of the tube with a sliding chromel−alumel thermocouple. The temperature increased linearly with distance from room temperature at the beginning of the hot zone to a temperature 80% of the way to the set point temperature at a distance of 6 cm and achieved the set point temperature a short distance into the remaining 10 cm of the hot zone before the viewing region.

In the present apparatus, the opportunity for thermalization and mixing of the O atom and fuel flows was better than in our previous work.[1] The distance from the microwave discharge source to the fuel injection point was ~0.6 m, providing extra opportunity for quenching of metastable species before mixing with the fuel. Location of the fuel injection position 16 cm upstream of the viewing region allowed ample time for mixing of the fuel and O atom flows. In C_2H_2 flames, visible emission from CH($A \rightarrow X$) and other minor species was seen to fill the

flowtube cross section ~3 cm downstream of the injector. The observation is in agreement with the calculated time of 7−10 ms (i.e., distance of 3−4 cm at a flow speed of 4 m/s) for molecular diffusion to spread fuel from the initial injected radial locations to the walls of the flowtube.

A 0.3 m f/5.3 McPherson folded-beam spectrometer was used to record the chemiluminescence signal through a 3.5 cm diam, f/5 calcium fluoride lens. Two 1200 line/mm gratings were used to cover the spectral region from 185 to 900 nm, one blazed at 200 nm and the other at 500 nm. The beam-folding mirrors in the spectrometer were coated with LiF to maximize UV reflectivity, and the spectrometer was continuously purged with dry nitrogen. The spectrometer was fitted with a Princeton Instruments optical multichannel analyzer (OMA), recording about 700 channels over an average 32.5 nm range. Continuous spectral plots were obtained by rotating the grating 25 nm with a stepper motor under computer control between each exposure. The two gratings were manually interchanged at 325 nm. Two long-pass interference filters were inserted at the appropriate wavelengths to prevent interference from second-order spectral components. Sixty signal spectra with fuel on and background spectra with fuel off were taken for each run covering the range from 185 to 900 nm.

The relative sensitivity of the spectrometer as a function of wavelength was calibrated from 300 to 900 nm using a standard tungsten filament lamp traceable to NIST data. The 185−300 nm wavelength range was calibrated with a deuterium lamp and found to be relatively flat until near the 185 nm cutoff of the OMA. Wavelength calibration was accomplished with a quartz-jacketed Hg pencil lamp in the UV and visible portions of the spectrum and with Ar emission lines from a plasma discharge in the near-IR. The wavelength accuracy was better than ±1 nm over the entire spectral range.

Matheson 99.994% purity Ar was used as the buffer gas. Acetylene was purchased as 2.0% in Ar from Matheson. Methane, ethane and ethylene were commercial purity and diluted to 2.0% in Ar in a stainless steel bomb prior to use. Carbon suboxide was prepared by dehydration of malonic acid with phosphorus pentoxide, as described previously.[1] The sequence of preparation and distillations used in our previous work was found to yield 50−60% C_3O_2, along with 40−50% CO_2. No additional attempts were made to remove CO_2, since in these experiments the residual CO_2 is an insignificant contributor with respect to combustion of the fuels, or quenching of CO(*a*). The C_3O_2/CO_2 mixture was diluted to 10% in Ar in a Pyrex bulb to facilitate accurate metering of the fuel flow.

2.2. Calibrations and Corrections. Since fuel and O atoms were partially consumed in the FFDS before reaching the spectrometer viewing position, it was necessary to correct the input flows for consumption and for temperature to obtain densities at the viewing position. The fuel+O reaction losses were integrated numerically from the injector position (assuming initial uniform mixing) to the viewing position, using the measured temperature profile to determine densities, flow speed, and reaction rate constants. For C_3O_2 fuel, one O atom was removed per fuel molecule reaction, corresponding to the main reaction channel, $C_3O_2 + O \rightarrow 3CO$. For C_2H_2, 2.3 O atoms were depleted per fuel molecule reaction, including the average additional 1.3 O atoms removed by the sequence of fast, branched reactions that follow the initial step. Table 1 shows the reaction rate constants used in the analysis.[12,15−18] Figure 2 shows the calculated species densities at the spectrometer viewing position as a function of temperature for typical sample flows of 570 sccm Ar, 1.2 sccm O, 2.4 sccm O_2, and either 0.18 sccm C_2H_2 or 0.29 sccm C_3O_2.

TABLE 1: Rate Constants Used in Data Analysis[a]

reaction	E/R (K)	A (cm^3 $molecule^{-1}$ s^{-1})	rate const
$C_3O_2 + O \rightarrow$ products	1070	1.67×10^{-11}	$A\ e^{-E/RT}$
$C_2H_2 + O \rightarrow$ products	1740	5.05×10^{-11}	$A\ e^{-E/RT}$
$CO(a) + O_2, O \rightarrow CO + O_2, O$[b]		2×10^{-10}	$A(T/295)^{1/2}$
$CO(a) + C_2H_2 \rightarrow CO + C_2H_2$		7.4×10^{-10}	$A(T/295)^{1/2}$

[a] References 12 and 15−19. [b] O and O_2 have similar rate constants (±10%).

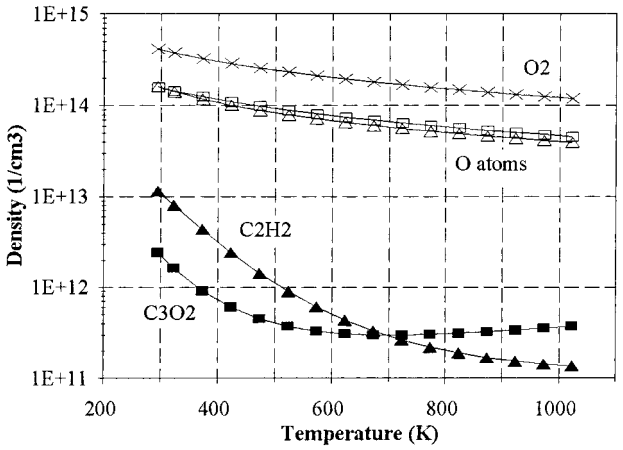

Figure 2. Calculated species number densities at spectrometer viewing position as a function of temperature. Results are for typical C_2H_2 (triangles) and C_3O_2 (squares) flames. Argon density (not shown) is 238 times the O_2 density.

It was also necessary to account for quenching of CO(*a*) by the species in the flowtube. The CO(*a*) state is long-lived (~7.6 ms)[19] and is strongly quenched by C_2H_2, O, O_2 and presumably also by C_3O_2, although no quenching rate constants are available for C_3O_2. For our conditions, quenching by Ar is more than 2 orders of magnitude slower than quenching by the other species.[19] Table 1 lists the quenching rate constants used in the data analysis. A temperature dependence proportional to the collision rate was used (i.e., $T^{1/2}$), based on measurements for a variety of quenchers in the 77−300 K range.[20] The rate constant for quenching by C_3O_2 was taken to be the same as for C_2H_2, although quenching by the fuel species is a minor factor. Possible quenching of the CO(*a*′), (*d*) and (*e*)states is considered with the data analyses in section 3.

Since pyrolysis of C_3O_2 could yield products that would react with O atoms to produce CO*, as well as alter the calculated fuel density in the spectrometer viewing region, we performed mass spectroscopic studies to look for dissociation of Ar-diluted C_3O_2 in the FFDS hot zone in the absence of oxygen atoms and molecules. An Extrel quadrupole mass spectrometer was installed to sample the flowtube gases 10 cm downstream of the hot zone via a length of fluoropolymer tubing. At room temperature, the C_3O_2 mass spectrometer signal was determined to vary linearly with the measured flow of fuel into the FFDS. When the flow was held constant and the FFDS heated, the C_3O_2 signal remained constant, even at temperatures up to 673 K, indicating excellent short-term stability of C_3O_2 in the hot zone.

3. Results

3.1. Acetylene Flame. The CO* band systems observed in the $C_2H_2 + O$ flame emission spectra are illustrated in Figures 3 and 4, which cover the UV and visible/near-IR spectral

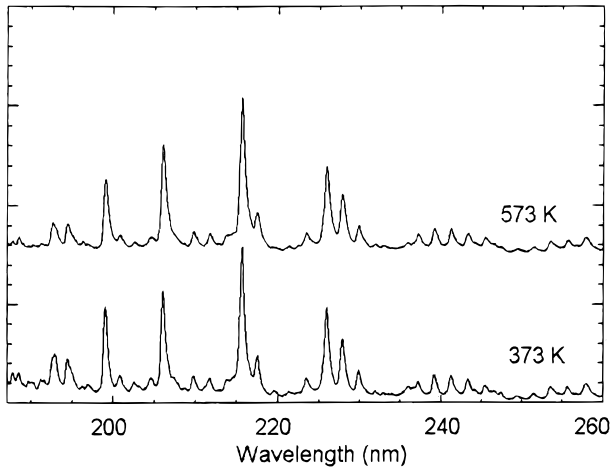

Figure 3. Ultraviolet emission spectra from C_2H_2 + O flame, showing Cameron band emissions, as well as dim Fourth Positive emissions below 192 nm. For comparison, the spectra have been offset and scaled to yield approximately the same intensity for different temperatures.

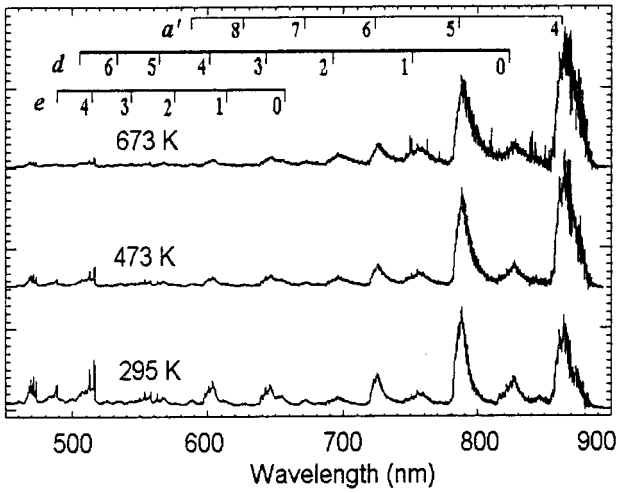

Figure 4. Visible/near-IR emission spectra from C_2H_2 + O flame, showing Herman, Triplet and Asundi bands, as well as C_2 Swan bands below 520 nm. For comparison, the spectra have been offset and scaled to yield approximately the same intensity for different temperatures. The (ν',0) vibrational assignments for the $e \rightarrow a$, $d \rightarrow a$ and $a' \rightarrow a$ systems are shown.

regions, respectively. For display purposes, the spectra in Figures 3 and 4 are offset and scaled so that the spectra have similar intensities at the different temperatures. The CO($a \rightarrow X$) Cameron band system dominates the UV portion of the spectrum, with the $\nu' \rightarrow \nu' - 2$, $\nu' - 1$, ν', $\nu' + 1$, $\nu' + 2$, $\nu' + 3$, and $\nu' + 4$ vibrational progressions proceeding to the red from wavelengths of approximately 192, 199, 206, 216, 226, 237, and 250 nm, respectively. At low temperatures, there is a trace of CO($A \rightarrow X$) Fourth Positive emission between 185 and 192 nm, particularly on the (1,6) vibrational transition at 186 nm. Between 280 and 450 nm, no significant emissions from CO* were observed, but strong CH($A \rightarrow X$) and ($B \rightarrow X$) and OH($A \rightarrow X$) emissions were seen. In the 460−520 nm region, the C_2($d \rightarrow a$) Swan bands are prominent at low temperatures, but decrease rapidly at higher temperatures relative to the CO* emissions. In the red and near-IR portions of the spectrum, the Herman ($e \rightarrow a$), Triplet ($d \rightarrow a$), and Asundi ($a' \rightarrow a$) band systems of CO are observed. Adjustment of the fuel flow, while maintaining a large excess of O atoms, yielded fuel reaction orders for the observed emission band systems from electronically excited CO, CH, OH, and C_2. The CO bands were all first order in fuel over the entire

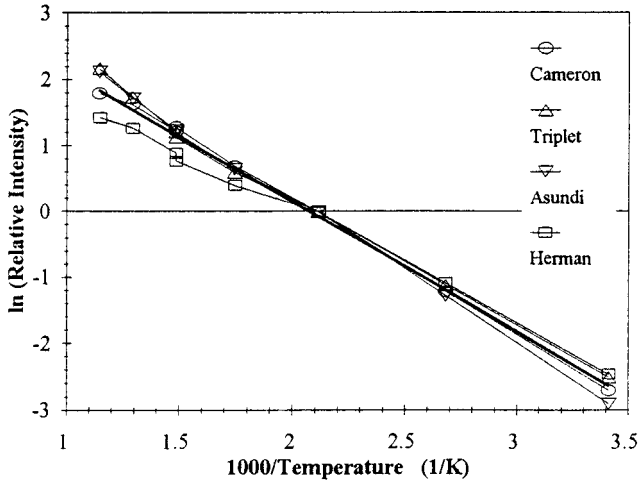

Figure 5. Arrhenius plots of the total band system relative intensities of Cameron, Herman, Triplet and Asundi systems in acetylene flame. For comparison, the relative intensities of each system are normalized to 1 at 473 K; the base e logarithm is plotted. The heavy line is the least-squares fit of an activation temperature.

temperature range. The apparent reaction order of the CH, OH, and C_2 bands was higher than first order and increased with temperature. The apparent order in fuel ranged between 1 and 2 for OH($A \rightarrow X$) and between 2 and 5 for CH($A \rightarrow X$). The order for CH($A \rightarrow X$) agrees with the production mechanism established by the group of Peeters[21] in dilute, low-pressure C_2H_2/O/H flames, where the total order in C_2H_2 and C_2H_2-derived H atoms would be 2−4 for the different contributing reaction sequences.

At each temperature, the total band system intensity of each of the four prominent CO* band systems was determined by summing the intensities of the individual vibrational components of the system. All band systems were essentially complete, except for the Asundi system, which included only the (4,0) and higher vibrational transitions. The total band system intensities at each temperature were then normalized by dividing by the calculated reactant concentrations (i.e., C_2H_2 and O atoms) at the spectrometer viewing position, and CO(a) emission was corrected for quenching. The resulting total band system relative intensities are shown in an Arrhenius plot in Figure 5. For comparison purposes, the intensities of each system have been multiplied by a factor that normalizes the system's intensity to 1 at 473 K. The total intensities of the Triplet, Cameron, and Asundi band systems have a very similar temperature dependence from room temperature through 873 K. The small deviation of the Herman band system intensity from the common trend at high temperature may be the result of incompletely resolving the Herman bands from the C_2 Swan bands, which change in intensity dramatically with temperature (Figure 4). We note that at room temperature the production rates of the CO(a'), (d) and (e) states in the O + C_2H_2 flame were determined to be in the ratio of 84:29:7 and that the CO(a) state production rate was essentially equal to the sum of the upper state rates, since the a state was produced entirely (within experimental uncertainty) by radiative cascade from those states.[1] Figure 5 shows that the rates of production of the a, a', d and e states remain essentially the same with respect to each other from room temperature up to 873 K (i.e., the slopes of the curves for each system are about the same).

The Arrhenius plots of the total band system relative intensities yield an apparent activation temperature (i.e., apparent activation energy divided by R) for the production of the CO triplet states. A least-squares fit to the data gives $E/R = 1970 \pm 300$ K and is indicated by the heavy line in Figure 5. The

result is a little higher than the value of 1740 K in Table 1 for the activation temperature of the first reaction step in acetylene combustion, $C_2H_2 + O \rightarrow$ products, but is within the combined experimental uncertainties. It is noted that over the wide temperature range of 195−2500 K the rate constant for the reaction, $C_2H_2 + O \rightarrow$ products, is best fit with a temperature-dependent Arrhenius preexponential factor;[12] however, in the 295−873 K range of interest, the simple two-parameter Arrhenius expression in Table 1 is an excellent fit.

In normalizing the band system intensities in Figure 5, a correction was applied for quenching of CO(*a*), but not the other triplet states. Although the radiative lifetimes of the *a*′, *d* and *e* states (~5 μs)[19] are 3 orders of magnitude shorter than the *a* state, it appears from a sparse collection of quenching rate constant data[19] that some quenching of these states may occur for our conditions. The available rate constants are inadequate for a detailed quenching correction, so we have estimated the effect of a "strong quenching" condition. Assuming that the quenching rates are much greater than the radiative rates of the *a*′, *d* and *e* states and that the quenching rate constants have a $T^{1/2}$ dependence, a correction was applied to the band system intensities analogous to the correction to the Cameron band intensities. The resulting Arrhenius slopes of the *a*′, *d* and *e* state band system intensities were slightly smaller than in Figure 5, giving a least-squares fit activation temperature of 1790 K, approximately 180 K less than the original fit. The best activation temperature probably lies between the uncorrected and "strong quenching" results.

The total band intensity data are most simply interpreted to suggest that the temperature dependence of the intensity of all of the triplet CO* band systems is due to the temperature dependence of the initial $C_2H_2 + O$ reaction step, and that the subsequent steps to produce CO* are relatively independent of temperature as to CO triplet state yield and distribution. The subsequent steps that are expected to generate CO* are very fast and are unlikely to kinetically limit the production rate of CO*. These observations, when combined with the conclusions of other work regarding the C_2O intermediate,[1,2,6] suggest that under dilute, low-pressure, fuel-lean conditions, C_2O is the major precursor to CO* over a broad range of temperature in the $C_2H_2 + O$ flame system and that the branching fractions for the reactions that produce C_2O and the relative CO* triplet yields from the $C_2O + O$ reaction are relatively temperature independent.

3.2. Carbon Suboxide. When C_3O_2 was used as fuel, spectra very similar to those obtained with C_2H_2 were recorded. At room temperature, however, emission from the C_3O_2 flame was too dim to accurately record, even with very long integration times. Above 350 K, the increase in CO* emission intensity with temperature was dramatic. This behavior appears to be due partly to the rapid reactive depletion of C_3O_2 and partly to increased branching to reaction r5b with increasing temperature (see below). Figures 6 and 7 show carbon suboxide flame emission spectra in the UV and visible/near-IR regions, respectively. The CO* triplet state emissions from the C_3O_2 flame appear to be vibrationally hotter than those from the C_2H_2 flame. The higher vibrational bands of the Triplet and Herman systems are significantly more pronounced with respect to the lower bands in the C_3O_2 flame spectra (Figure 7) than in the C_2H_2 flame spectra (Figure 4), although the highest bands are slightly obscured by overlap with CH and C_2 emissions in the C_2H_2 spectra. Also, CO(*A*→*X*) Fourth Positive bands are seen just inside the 185 nm cutoff of the OMA in the C_3O_2 spectra,

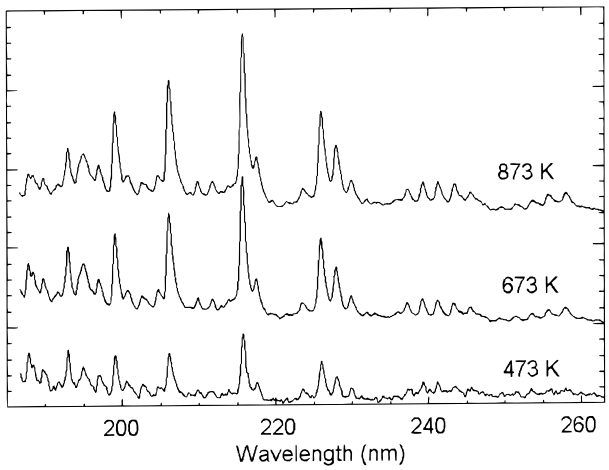

Figure 6. Ultraviolet emission spectra from $C_3O_2 + O$ flame. For comparison, the spectra have been offset and scaled to yield approximately the same intensity for different temperatures.

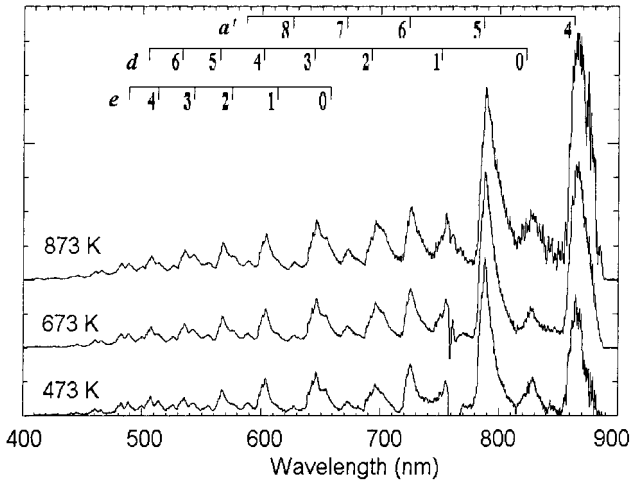

Figure 7. Visible/near-IR emission spectra from $C_3O_2 + O$ flame. For comparison, the spectra have been offset and scaled to yield approximately the same intensity for different temperatures. The (v',0) vibrational assignments for the *e*→*a*, *d*→*a* and *a*′→*a* systems are shown. A distortion near 762 nm is due to O_2(*b*→*X*) background emission.

whereas the same bands are barely observable in the analogous C_2H_2 flame spectra.

Figure 8 is an Arrhenius plot of the total band system relative intensities of CO* triplet emission from the $C_3O_2 + O$ flame. The spectral data were summed to get total band system intensities, normalized to reactant concentrations in the viewing region, and corrected for quenching of CO(*a*) in the same way as the acetylene spectra, using the same band integrations. For comparison purposes in Figure 8, the intensities of each system have been multiplied by a factor that normalizes the system's intensity to 1 at 473 K. An apparent activation temperature can be derived for production of CO* in the *a*′, *d* and *e* triplet states, which display essentially the same relative behavior with temperature. A least-squares fit gives the value $E/R = 3040 \pm 300$ K in the temperature range 373−873 K and is indicated by the heavy line in Figure 8. If the *a*′, *d* and *e* state emissions are corrected with a "strong quenching" approximation, analogous to the procedure described for the C_2H_2 data, the fit gives an activation temperature of 2780 K. The relative production rates of the *a*′, *d* and *e* states with respect to each other are essentially the same at high temperature as at room temperature. The intensity of the Cameron band system (excluded from the fit) appears to increase a little more rapidly with temperature than

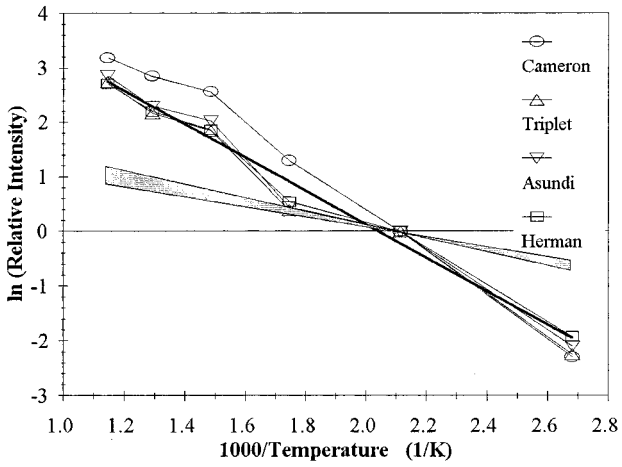

Figure 8. Arrhenius plots of the total band system relative intensities of the Cameron, Herman, Triplet and Asundi systems in carbon suboxide flame. For comparison, the relative intensities for each system are normalized to 1 at 473 K; the base e logarithm is plotted. The heavy line is the least-squares fit of an activation temperature (neglecting Cameron). The shaded region is the range of activation temperatures reported for the C_3O_2 + O reaction at low to moderate temperature.

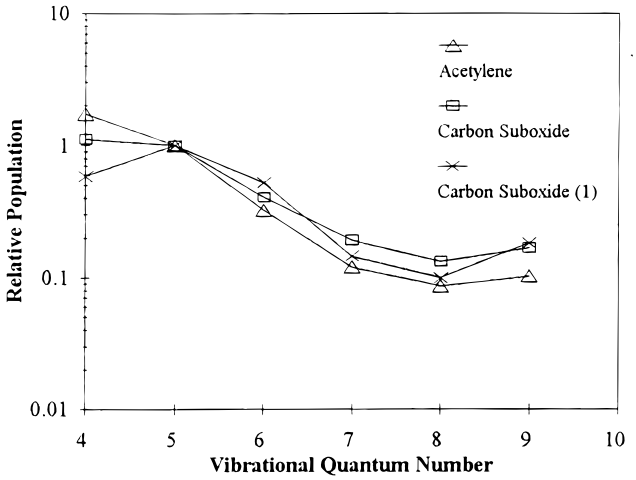

Figure 9. Relative vibrational level populations of CO(a') typical of the 473−873 K temperature range. "Carbon suboxide (1)" refers to the result at room temperature with the fuel injection point located 1 cm upstream of the spectrometer viewing position. Populations are normalized to 1 at $v' = 5$.

the Herman, Triplet, and Asundi band systems. It is unlikely that this indicates a difference in quenching of CO(a) by C_2H_2 and C_3O_2, which is estimated to be relatively unimportant compared with quenching by O and O_2 (Figure 2 and Table 1). A possible explanation could be the thermal activation of another minor chemical pathway that populates CO(a) in the C_3O_2 flame.

The apparent activation temperature for CO* emission is much greater than the activation temperature of 1070 ± 165 K for the initial reaction, C_3O_2 + O → products, deduced from rate constant measurements in the 250−450 K temperature range.[15,18] The range of Arrhenius slopes implied by the reported activation energy of the initial reaction is shown as a shaded region in Figure 8, anchored to a relative intensity value of 1 at 473 K for comparison purposes. Since the CO* activation temperature is much larger than the value observed for CO* emission from C_2H_2 + O, which also presumably involves C_2O + O as the main chemiluminescent step, it is unlikely that it is associated with the C_2O + O reaction. A possible explanation is that the activation temperature measured for the initial reaction at lower temperatures is inaccurate, although the reported uncertainty is small. Another possible explanation is a large activation temperature for the branch of the C_3O_2 + O reaction that produces C_2O.

We consider here the possibility that the measured activation temperature describes reaction r5b. Because the rate constant for reaction r5b implied by our measured activation temperature and a room-temperature branching fraction of a few percent becomes comparable to the presumed total reaction rate constant (Table 1) at high temperature, a correction to our procedure for calculating species densities at the viewing position is required. An iterative solution to expressions for k_{5a} and k_{5b} was performed, subject to the constraints imposed by the measured value of $k_5 = k_{5a}+k_{5b}$ in the 250−450 K range, a room-temperature branching fraction k_{5b}/k_5 of approximately 1%−3%, and our measured activation temperature for k_{5b}. Expressions for k_{5a} and k_{5b} were postulated, and species densities were calculated at the viewing position, followed by an Arrhenius fit to the band system intensities (corrected by the new species densities) to obtain a new activation temperature for k_{5b}. The iteration was repeated and converged toward the approximate solutions, $k_{5a} = 1.2 \times 10^{-11} \exp(-900/T)$ and $k_{5b} = 2.7 \times 10^{-11} \exp(-2500/T)$. The corresponding total reaction rate constant is well fit in the 250−450 K range by the expression, $k_5 = 1.4 \times 10^{-11} \exp(-933/T)$, which is within uncertainty limits of the measured value.[15,18] At 295 K, k_{5b}/k_5 is 0.01, comparable to the low end of the range of reported values.[10,15] The activation temperature of 2500 K for k_{5b} agrees with the value of ~2700 K that results from the iterated Arrhenius fit to the intensity data. The derived rate constant expressions imply a large increase with temperature for the branching fraction k_{5b}/k_5, reaching a value of 0.26 at 873 K.

3.3. Comparison of C_2H_2 + O and C_3O_2 + O Flame Spectra. To quantitatively compare the CO triplet state vibrational distributions for C_2H_2 and C_3O_2 flames, the (v',0) vibrational bands within a given band system were individually integrated and converted to a relative upper vibrational level population with the equation

$$P_{v'} = I_{v',0}\left[\frac{\upsilon^3_{v',0} q_{v',0}}{\sum_{v''} \upsilon^3_{v',v''} q_{v',v''}}\right]^{-1}$$

where $P_{v'}$ is the relative population of the v' upper level, $I_{v',0}$ is the integrated intensity of the (v',0) transition, $\nu_{v',v''}$ is the frequency of the (v',v'') transition, $q_{v',v''}$ is the Franck−Condon factor,[1] and the sum is over all v'' lower states. The (4,0) Asundi band was close to the OMA cutoff wavelength, resulting in more uncertainty in the relative population of the a', $v' = 4$ level. Figures 9 and 10 show the relative vibrational level populations of the CO(a') and (d) states, respectively, for both the C_2H_2 and C_3O_2 flames. For display purposes, the relative vibrational populations derived for the two fuels are normalized to the $v' = 5$ result in the Asundi ($a' \rightarrow a$) system (Figure 9) and to the $v' = 0$ result in the Triplet ($d \rightarrow a$) system (Figure 10). Higher vibrational levels of the Asundi and Triplet systems, as well as the entire Herman ($e \rightarrow a$) system, were not included in the comparisons, due to overlap with other CO* emissions and with C_2 Swan bands in the C_2H_2 flame. Aside from small differences near the uncertainty level, the vibrational distributions were relatively independent of temperature over a range of high temperatures. Therefore, the data from the higher temperature runs were pooled, and the results shown in Figures 9 and 10 are actually average relative vibrational population distributions

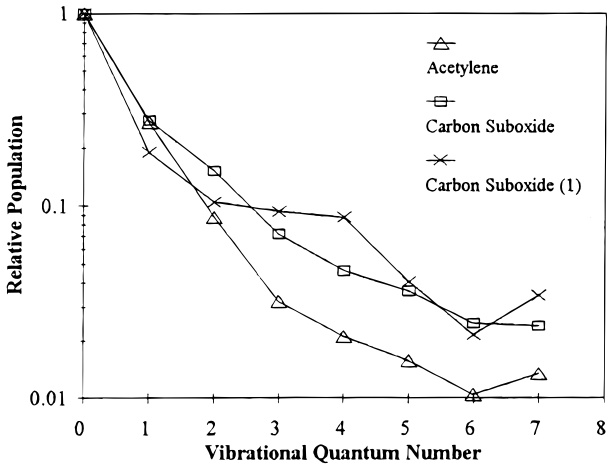

Figure 10. Relative vibrational level populations of CO(*d*) typical of the 473−873 K temperature range. "Carbon suboxide (1)" refers to the result at room temperature with the fuel injection point located 1 cm upstream of the spectrometer viewing position. Populations are normalized to 1 at $v' = 0$.

over the temperature range of 473 to 873 K. For both fuels, the vibrational distributions in Figures 9 and 10 are a little hotter than the distributions measured in our previous work at room temperature,[1] possibly due to the extra thermal energy available to the reactants in the higher temperature experiments.

A few additional experiments were performed at room temperature on the $C_3O_2 + O$ flame with the fuel injector located 1 cm upstream of the spectrometer viewing position, instead of at the normal location 16 cm upstream of the spectrometer. This arrangement simulates the conditions of our previous room-temperature experiments in a different apparatus where the spectra were recorded from a region 1−3 cm downstream of the fuel injection point. With the same flows as in other experiments reported here, the entire spectral signature of CO* was observed at room temperature. The CO(*a*′) and (*d*) vibrational populations derived with the injector located 1 cm upstream of the spectrometer are included in Figures 9 and 10, labeled "Carbon Suboxide (1)". On average, the vibrational distributions in the *a*′ and *d* states are very similar to those observed at high temperatures with the injector located 16 cm upstream.

The relative vibrational populations of the CO(*a*) state are not included in the comparisons in Figures 9 and 10, but were essentially identical for the two fuels and independent of temperature (e.g., Figures 3 and 6). The vibrational populations in the *d* state (and to a lesser extent the *a*′ state), however, appear somewhat hotter in the $C_3O_2 + O$ flame spectra. The difference between the Cameron emission and the other triplet emissions may reflect the different dominant population mechanisms of the triplet states. At room temperature[1] and probably at higher temperatures, the CO(*a*) state is populated almost entirely via radiative emission from higher triplet states involving highly nondiagonal Franck−Condon factors. The resulting vibrational distribution in the *a* state may not reflect very strongly the vibrational distributions in the upper electronic states of the radiative transitions. The *a*′ and *d* states, however, are populated directly in the chemical reaction, and thus their vibrational distributions would be more sensitive to the internal energy of the C_2O precursor. The C_2O may be more highly vibrationally excited in the carbon suboxide flame due to the higher exothermicity of the $C_3O_2 + O$ reaction, compared with the reactions that generate C_2O in the acetylene flame. The exothermicity to ground electronic states of the $C_3O_2 + O \rightarrow C_2O + CO_2$ reaction (i.e., −39.3 kcal/mol, based on $\Delta H^o_{f,298}$= 92 kcal/mol for C_2O)[2,8] is larger than the exothermicity of the $C_2H_2 + O \rightarrow C_2O + H_2$ reaction (i.e., −21.8 kcal/mol),[2,8] or the $HCCO + O \rightarrow C_2O + OH$ reaction (i.e., −1 kcal/mol),[2,8,22] which are the postulated sources of C_2O in the acetylene flame. Extra internal energy deposited in C_2O could be passed to CO* in the subsequent $C_2O + O$ reaction. The enhanced presence of CO($A \rightarrow X$) Fourth Positive emission in the C_3O_2 flame is also consistent with a more energetic CO*. The CO(*A*) state is apparently populated via intersystem crossing from high-lying triplet states,[23,24] and only CO(*e*) and CO(*d*, v > 3) states are energetic enough for this transfer to occur.[25]

Chemiluminescence from O atom flames with methane (CH_4), ethane (C_2H_6) and ethylene (C_2H_4) was also briefly investigated. Tjossem and Cool[3] have reported the detection of the C_2O radical in several light hydrocarbon/O_2/Ar flames at low pressure, using multiphoton ionization techniques. On the basis of the presence of C_2O, the detection of CO* emissions from these fuels might reasonably be expected, although to our knowledge, these emissions have not been previously reported, at least under very fuel-lean conditions. Because of the slow reaction of O with CH_4 and C_2H_6, the emission was weak, but Cameron bands were clearly observed above temperatures of ∼600 K for our typical fuel and O atom concentrations. Cameron, Asundi, and Triplet emissions were observed from C_2H_4 flames at temperatures above 373 K, with a CO(*a*) vibrational distribution similar to that of the acetylene and carbon suboxide flames.

4. Summary and Conclusions

A comparison of CO* triplet state yields and vibrational populations was used in previous work to infer that the same reaction is responsible for CO* formation in dilute, low-pressure, fuel-lean flames of C_3O_2 and C_2H_2 with O atoms at room temperature.[1,2] Specifically, the $C_2O + O$ reaction appeared to be the main source of CO* for both fuels. Essentially the same relative triplet state yields and vibrational level distributions in the upper states were observed for both fuels in the Cameron, Asundi, Triplet and Herman band systems.

In the present study, we have examined the temperature dependence of the previous observations. The close similarity of the C_3O_2 and C_2H_2 flame emission spectra at high temperature was consistent with previous work at room temperature. For both fuels, the relative yields of the *a*, *a*′, *d*, and *e* triplet states with respect to each other remained essentially constant throughout the 295−873 K temperature range. At high temperatures, the vibrational distributions in the triplet states were also similar to the room-temperature results. These observations support the conclusion that the same precursor (i.e., C_2O) is the main source of CO* throughout the temperature range.

In the acetylene flame, our measured activation temperature for production of each of the CO* triplet states was essentially the same and was very close to the accurate value reported for the initial reaction, $C_2H_2 + O \rightarrow$ products. It is therefore concluded that the overall production rate of CO* is controlled by the initial reaction step and that branchings in the subsequent steps that lead to the triplet states of CO are relatively temperature independent. This observation is consistent with the conclusion that the main CO* production mechanism is the $C_2O + O$ reaction throughout the temperature range, as appears to be the case at room temperature,[1] and that the relative triplet state yields in the reaction are essentially independent of temperature.

In the carbon suboxide flame, although the relative CO* triplet yields and upper state vibrational populations were nearly

independent of temperature, the observed activation temperature for production of the triplet states was found to be much greater than the value reported at moderate temperatures for the initial reaction, $C_3O_2 + O \rightarrow$ products. This result suggests that C_2O remains the main CO* precursor at high temperatures, but that the minor reaction branch that produces C_2O may have a higher activation energy than the major branch of the initial reaction. By this interpretation, the activation temperature for the reaction, $C_3O_2 + O \rightarrow C_2O + CO_2$, would be ~2.5 times larger than the value reported in the low end of our temperature range for the total reaction, $C_3O_2 + O \rightarrow$ products (i.e., ~2500 K vs ~1000 K). Further investigation of the reaction rates of the separate branches of the $C_3O_2 + O$ reaction is necessary at high temperature.

At high temperatures, the CO(*d*) (and possibly *a*′) state vibrational populations were somewhat hotter with C_3O_2 fuel than with C_2H_2, in accord with previous room temperature observations.[1] In addition, the C_3O_2 flames exhibited distinct CO Fourth Positive emission at all temperatures, whereas the C_2H_2 flames showed only traces of these emissions at low temperatures, which disappeared altogether at higher temperatures. These observations are also consistent with C_2O as the precursor to CO* throughout the temperature range, since C_2O (and subsequently its CO* daughter product) can be formed with more internal energy in the C_3O_2 flame.

Emissions from OH($A \rightarrow X$), CH($A \rightarrow X$) and ($B \rightarrow X$), and C_2-($d \rightarrow a$) were observed in the acetylene flame as a function of temperature and fuel concentration. The intensities of these emissions decreased rapidly with increasing temperature relative to the CO* emission, and exhibited higher than first-order dependence on fuel concentration. Although C_2 is a potential source of CO triplet and Fourth Positive emission in reactions with O_2,[24,26,27] these reactions do not appear to be a major source of CO* in dilute acetylene/O atom flames when O and O_2 densities are comparable.

Acknowledgment. This work was supported through the Air Force Research Laboratory, Edwards AFB, T. A. Smith, project manager. The authors thank T. A. Smith (AFRL), W. L. Dimpfl (Spectral Sciences, Inc.), and M. L. Burke for helpful discussions.

References and Notes

(1) Burke, M. L.; Dimpfl, W. L.; Sheaffer, P. M.; Zittel, P. F.; Bernstein, L. S. *J. Phys. Chem.* **1996**, *100*, 138.
(2) Becker, K. H.; Bayes, K. D. *J. Chem. Phys.* **1968**, *48*, 653.
(3) Tjossem, P. J. H.; Cool, T. A. *Symp. (Int.) Combust. [Proc.]* **1984**, *20*, 1321.
(4) Marmo, F. F.; Pardur, J.; Warneck, P. *J. Chem. Phys.* **1966**, *47*, 1438.
(5) Peeters, J.; Boullart, W.; Langhans, I. *Int. J. Chem. Kinet.* **1994**, *26*, 869.
(6) Becker, K. H.; Horie, O.; Schmidt, V. H.; Wiesen, P. *Chem. Phys. Lett.* **1982**, *90*, 64.
(7) Walch, S. P. *J. Chem. Phys.* **1980**, *72*, 5679.
(8) JANAF Thermochemical Tables, 3rd ed. *J. Phys. Chem. Ref. Data* **1985**, *14*, Supplement 1.
(9) Williamson, D. G.; Bayes, K. D. *J. Phys. Chem.* **1969**, *73*, 1232.
(10) Williamson, D. G.; Bayes, K. D. *J. Am. Chem. Soc.* **1967**, *89*, 3390.
(11) Becker, K. H.; Kley, D.; Norstrom, R. J. *Symp. (Int.) Combust. [Proc.]* **1968**, *12*, 405.
(12) Michael, J. V.; Wagner, A. F. *J. Phys. Chem.* **1990**, *94*, 2453.
(13) Boullart, W.; Peeters, J. *J. Phys. Chem.* **1992**, *96*, 9810.
(14) Peeters, J.; Boullart, W.; Devriendt, K. *J. Phys. Chem.* **1995**, *99*, 3583.
(15) Pilz, C.; Wagner, H. *Z. Phys. Chem. (Frankfurt/Main)* **1974**, *92*, 323.
(16) DeMore, W. B.; Sander, S. P.; Golden, D. M.; Hampson, R. F.; Kurylo, M. J.; Howard, C. J.; Ravishankara, A. R.; Kolb, C. E.; Molina, M. J. *Chemical Kinetics and Photochemical Data for use in Stratospheric Modeling*; JPL Publication 92-20; Jet Propulsion Laboratory: Pasadena, CA, 1992.
(17) Mallard, W. G.; Westley, F.; Herron, J. T.; Hampson, R. F.; Frizzel, D. H. *NIST Chemical Kinetics Database—Ver. 2Q98*; National Institute of Standards and Technology: Gaithersburg, MD, 1998.
(18) Liuti, G.; Kunz, C.; Dondes, S. *J. Am. Chem. Soc.* **1967**, *89*, 5542.
(19) Schofield, K. *J. Phys. Chem. Ref. Data* **1979**, *8*, 723.
(20) Clark, W. G.; Setser, D. W. *Chem. Phys. Lett.* **1975**, *33*, 71.
(21) Devriendt, K.; Peeters, J. *J. Phys. Chem. A* **1997**, *101*, 2546.
(22) Oakes, J. M.; Jones, M. E.; Bierbaum, V. M.; Ellison, G. B. *J. Phys. Chem.* **1983**, *87*, 4810.
(23) Fontjin, A.; Johnson, S. E. *J. Chem. Phys.* **1973**, *59*, 6193.
(24) Fontijn, A.; Randall, M. Y.; Goumri, A.; Brock, II, P. E. *34th AIAA/ASME/SAE/ASEE Joint Propulsion Conference and Exhibit [Proc.]*, **1998**, AIAA98−3538.
(25) Huber, K. P.; Herzberg, G. *Molecular Spectra and Molecular Structure, IV. Constants of Diatomic Molecules*; Van Nostrand Reinhold: New York, 1979.
(26) Reisler, H.; Mangir, M. S.; Wittig, C. *Chem. Phys.* **1980**, *47*, 49.
(27) Filseth, S. V.; Hancock, G.; Fournier, J.; Meier, K. *Chem. Phys. Lett.* **1979**, *61*, 288.